

DreamCom: Finetuning Text-guided Inpainting Model for Image Composition

Lingxiao Lu, Bo Zhang, Li Niu

Department of Computer Science and Engineering, MoE Key Lab of Artificial Intelligence,
Shanghai Jiao Tong University

{lulingxiao,bo-zhang,ustcnewly}@sjtu.edu.cn

Abstract

The goal of image composition is merging a foreground object into a background image to obtain a realistic composite image. Recently, generative composition methods are built on large pretrained diffusion models, due to their unprecedented image generation ability. They train a model on abundant pairs of foregrounds and backgrounds, so that it can be directly applied to a new pair of foreground and background at test time. However, the generated results often lose the foreground details and exhibit noticeable artifacts. In this work, we propose an embarrassingly simple approach named DreamCom inspired by DreamBooth. Specifically, given a few reference images for a subject, we finetune text-guided inpainting diffusion model to associate this subject with a special token and inpaint this subject in the specified bounding box. We also construct a new dataset named MureCom well-tailored for this task.

1. Introduction

Image composition [34] aims to produce a high-quality composite image by combining the foreground and background from different image sources, which has a wide range of applications including artistic creation, E-commerce, data augmentation. Early works [20, 44, 52] decompose image composition into different sub-tasks (e.g., image blending, image harmonization) to solve different issues (e.g., unnatural boundary, inharmonious illumination) existing in the composite image. To obtain a realistic composite image by addressing all these issues, multiple sub-tasks need to be performed sequentially. Such multi-stage processing is very cumbersome and thus hinders real-world applications.

Recently, some works [28, 43, 48] attempt to solve all the issues with one unified diffusion model, which can accomplish end-to-end image composition. Given a foreground image and a background image with a bounding box speci-

fying the foreground placement, they could directly produce the final composite image with the foreground seamlessly and naturally placed in the bounding box. These methods can be roughly categorized into two groups: **object-to-object mapping and token-to-object mapping conditioned on background with bounding box**.

The first group of methods (e.g., PbE [48], Object-Stitch [43], ControlCom [50]) learn object-to-object mapping conditioned on background with bounding box. They train a diffusion model based on massive triplets of foregrounds, backgrounds with bounding boxes, and real images, so that it can be directly applied to a new pair of foreground and background with bounding box to produce a composite image at test time. However, the generated results often fail to preserve the details of foreground object. Additionally, these methods only use one foreground image, lacking the ability to take advantage of multiple reference images for the same subject. This shortcoming greatly limits their extendability, because multiple foreground images could provide complementary useful information, especially for different viewpoints.

The second group of methods [28] learn token-to-object mapping conditioned on background with bounding box. They finetune a pretrained diffusion model on a few reference images of one subject, which enables compositing this subject into other background images. For example, DreamEdit [28] first finetunes a pretrained text-to-image generation model on a few reference images of one subject to associate this subject with one special token, which is the same as DreamBooth [39]. Then, they segment the generated foreground and combine it with the background through the diffusion process. The above procedure is repeated several times for better visual effect. DreamEdit relies on segmentation and iterative composition at test time, which is very tedious. Moreover, the foreground generation process is not conditioned on the background image, so the geometric and semantic compatibility between foreground and background cannot be guaranteed.

Our work belongs to the second group and proposes a more compact solution than DreamEdit [28]. We fine-

Work in progress.

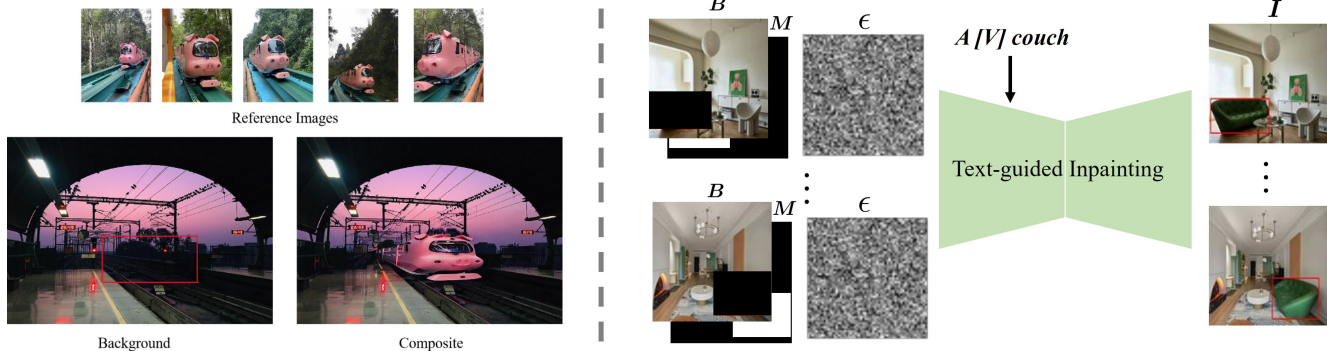


Figure 1. (a) The left subfigure illustrates our task. Given a background with a bounding box and multiple reference images of a subject, we aim to produce a composite image, in which the subject is seamlessly and reasonably placed in the bounding box. (b) The right subfigure illustrates our network. We finetune a text-guided inpainting model using multiple reference images of a subject, in which the text prompt contains a special token “[V]” associated with this subject.

tune text-guided inpainting model on a few reference images of one subject. In other words, we inpaint the subject in the bounding boxes of these reference images using text prompts. Specifically, we first obtain the bounding box masks as inpainting masks based on the bounding boxes of this subject. The denoising U-Net takes the masked background, bounding box mask, and noisy image as input, text prompt containing a special token as injected condition, to recover the complete ground-truth image. In this way, the model associates this subject with a special token and generates this subject compatible with background in the bounding box. At test time, given a new background with a bounding box, we apply the finetuned model to generate this subject in the bounding box. Compared with [28], our method does not require segmentation and iterative composition. More importantly, the foreground generation process is conditioned on background image, so the generated foreground has higher chances to be compatible with the background in terms of geometry and semantics.

We conduct experiments on DreamEditBench dataset released by [28], which only has 220 background images and 30 subjects for 15 categories. To supplement this dataset, we construct a new dataset named **Multi-reference Composition** (MureCom), which has 640 background images and 96 subjects for 32 categories. The major contributions of our work can be summarized as follows: 1) We propose a simple yet effective image composition baseline based on text-guided inpainting diffusion model. 2) We contribute a new dataset MureCom to supplement the existing DreamEditBench dataset.

2. Related Work

2.1. Image Composition

A composite image could be easily acquired by splicing the foreground object from one image and pasting it

on another background image, but the obtained composite image could be of poor quality due to the inconsistency between foreground and background. The inconsistency include appearance inconsistency, geometry inconsistency, and semantic inconsistency, as discussed in [34].

For appearance inconsistency, image blending [35, 51, 52] worked on addressing the unnatural boundary so that the foreground is seamlessly blended into the background. Image harmonization [4, 8–10, 14–17, 21, 22, 29, 31, 33, 37, 42, 44, 45, 47] studied on adjusting the foreground illumination to create a harmonious composite image. Moreover, shadow generation [20, 32, 41] attempted to generate plausible shadow on the background for the inserted foreground.

For geometry and semantic inconsistency, object placement [26, 53] aimed to predict the reasonable location and scale of foreground given a pair of foreground and background. To further cope with inconsistent camera viewpoint, previous spatial transformation methods [6, 30, 49] proposed to forecast the warping parameters to correct the foreground geometrically. Nevertheless, the predicted warping parameters can only realize affine or perspective transformation, which is unable to handle complicated geometric adjustment (e.g., dramatically changed viewpoint, non-rigid foreground objects).

Early works on image composition usually only focus on one sub-task or performs multiple sub-tasks sequentially. Recently, generative image composition [23, 43, 48] proposed to solving all the issues by using one unified model. As discussed in Section 1, the results generated by [43, 48] are not faithful to the input foreground. The method in [28] requires segmentation and iterative composition, which is very tedious.

2.2. Subject-driven Image Generation and Editing

Subject-driven image generation refers to generating images with specific subjects, while subject-driven image edit-

ing refers to replacing or inserting specific subjects into background images. GAN-based works [3, 40, 52] on subject-driven editing proposed to generate specific subjects by manipulating the latent representations in the generator. With the rapid development of diffusion models, text-guided subject-driven image generation [11, 24, 39] has attracted increasing research interest. They proposed to leverage multiple customized images of for concept learning and embed the concept into text prompts, so that the images with specified concept can be generated based on the text prompts. Some other works [12, 46] proposed to extract the representation of customized images using encoders. These subject-driven image generation methods cannot be directly applied to our task, because they cannot use the provided background and control the foreground placement. Additionally, some works on text-guided subject-driven image editing [7, 13, 27] proposed to replace the objects in the background images based on pretrained diffusion model.

It can be seen that lots of works have been done for various types of image generation and editing tasks based on diffusion model. In this work, we focus on generative image composition [23, 28, 43, 48], which targets at a realistic composite image given a background image with a bounding box and a foreground image.

3. Preliminary

Our method is built upon the Stable Diffusion (SD) [38] model tailored for text-guided image inpainting. SD is a latent diffusion model consisting of an auto-encoder and a denoising U-Net, which are trained in two stages. In the first stage, the SD model trains the auto-encoder, in which the encoder \mathcal{E} projects images I into latent space $z_0 = \mathcal{E}(I)$ and then the decoder \mathcal{D} reconstructs the original images $\hat{I} = \mathcal{D}(z_0)$. The trained auto-encoder is fixed and provides latent space for the second stage.

In the second stage, the SD model trains the denoising U-Net ϵ_θ [19] in the latent space from the first stage. In particular, T -step noise is added to latent space feature z_0 to produce $z_t; t = 1, 2, \dots, T$. Then, the denoising U-Net is trained using the following latent denoising loss:

$$\mathcal{L}_{LDM} := \mathbb{E}_{\epsilon \sim \mathcal{N}(0,1), t} \left[\|\epsilon - \epsilon_{\theta_1}(z_t, t, \mathbf{M}, \mathbf{b}, \tau_{\theta_2}(y))\|_2^2 \right], \quad (1)$$

where $\epsilon \sim \mathcal{N}(0, 1)$ is the Gaussian noise added to the latent space feature z_0 in each step, ϵ_{θ_1} is the denoising U-Net that predicts the noise ϵ in the current step t . y is the text prompt and τ_{θ_2} is the text encoder that projects the text prompt into token embeddings. \mathbf{M} is the inpainting mask indicating the regions to be inpainted. $\mathbf{b} = \mathcal{E}(\mathbf{B})$ is the latent feature map of masked background \mathbf{B} , which is obtained by removing the content within the mask in I . The denoising U-Net ϵ_{θ_1} takes $z_T, t, \mathbf{M}, \mathbf{b}$, and y as input, to estimate the noise at step T . Specifically, z_T, \mathbf{M} , and \mathbf{b} are concate-

nated channel-wisely, leading to 9-channel input tensor for the denoising U-Net. $\tau_{\theta_2}(y)$ is injected into the transformer block in U-Net via cross-attention.

During inference, we sample random Gaussian noise as initial z_T . The denoising U-Net ϵ_{θ_1} estimates the noise at step T . This procedure is iteratively executed to estimate the noise at each denoising step t , so that the latent feature map is gradually denoised and recovers the noise-free latent feature map z_0 . Finally, z_0 is sent into the decoder \mathcal{D} to produce the image. For more details about the training and inference of Stable Diffusion, please refer to [38].

4. Our Method

The pretrained diffusion model in Section 3 can fill in the masked region according to the text prompt. In this section, we adapt the diffusion model to generate a specific subject in the masked region. Inspired by [39], we insert a rarely used token [V](*e.g.*, *sks*) into the text prompt and associate this token with a specific subject, by finetuning the pretrained diffusion model on a few (*e.g.*, 3, 5) references images of this subject. For example, when the subject is a couch, the text prompt y could be “A *sks* couch”. In our task, the inpainting mask \mathbf{M} is the bounding box mask of the subject in each reference image. The masked background \mathbf{B} is obtained by erasing the content within the bounding box in each reference image. Then, we finetune the pretrained diffusion model using the loss function in Eqn. 1.

To enrich the limited training set (*e.g.*, 3 ~ 5 reference images), we perform data augmentation, including horizontal flipping and random cropping. In addition to these, to better adapt to our inpainting task, we also apply scaling transformation as an augmentation technique. During the scaling transformation, the same operations are applied to the mask.

After finetuning the diffusion model, given a new background image with a bounding box, we can get \mathbf{M} and \mathbf{B} . By using the text prompt y containing the special token, we start from random Gaussian noise $z_T \sim \mathcal{N}(0, 1)$ and produce the composite image through the denoising process.

One practical issue is that the pretrained inpainting diffusion model we use is trained with global text prompt, *i.e.*, the text prompt is the description of the whole image instead of the masked region. If we use the description of inpainted object as text prompt, when the bounding box is very small, the model is prone to generate nothing in the bounding box. The recent work [2] is a text-guided inpainting model with local text prompt, which perfectly satisfies our requirement, but this work is not open-sourced. As a remedy, we find that it is helpful to crop a local region surrounding the bounding box as the new background image, when the bounding box

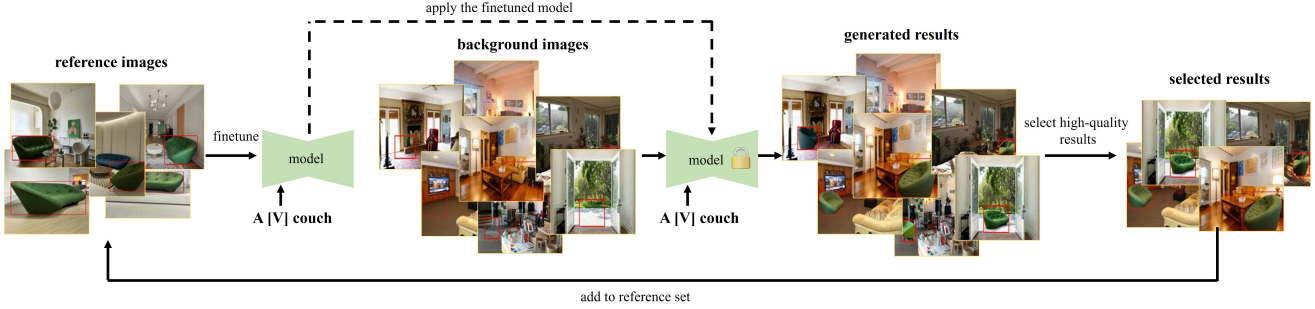


Figure 2. A human-in-the-loop pipeline for continual model enhancement.

is very small. One empirical observation is that the model can usually generate satisfactory results when the ratio of bounding box area over the entire image area is larger than 25%. Therefore, when the bounding box ratio is smaller than 25%, we get the cropped image in which the bounding box is at center and the bounding box ratio is 25%. Then, we generate the composite image based on the cropped image.

Another observation is that the performance of finetuned model is not very stable, but the optimal results obtained by sampling multiple times are usually of high quality. Therefore, in practice, we can employ a human-in-the-loop pipeline as shown in Figure . Provided with a small set of reference images, we finetune the model with the reference set and apply the finetuned model to more background images. Then, we manually select the high-quality results and add them to the reference set. We can repeat this procedure to continually improve the model.

5. Dataset Construction

The work [28] provides DreamEditBench dataset, offering a total of 440 background images, out of which 220 background images are suitable for our task. The reference images corresponding to the backgrounds in this dataset are sourced from the Dreambooth dataset [39]. There are 30 subjects for 15 categories, in which each subject has a few (3 ~ 5) reference images. Among them, some subjects within the same category share a common background set, while the remaining subjects have their own unique background set. There are a total of 22 background sets, each consisting of 10 images. Thus, there are in total $300 = 30 \times 10$ subject-background pairs.

To enrich the diversity of DreamEditBench dataset, we construct a new dataset named **Multi-reference Composition** (MureCom). First, we collect 640 background images from R-FOSD dataset [1], in which each background image is associated with one category from a list of 32 categories and a manually annotated bounding box suitable for placing an object from this category. Then, for

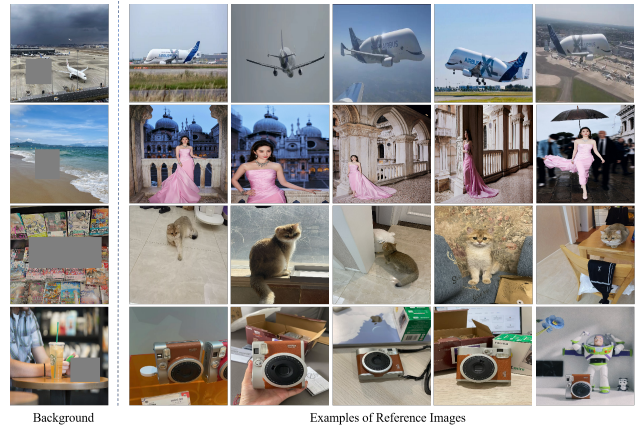


Figure 3. Several examples from our MureCom dataset. In each example, we show one background image with bounding box, and also show five reference images of one subject belonging to this category.

each of 32 categories, we collect 3 subjects with 5 reference images for each subject from the Internet. Since each category has 20 background images and 3 subjects, we can have in total $1,920 = 32 \times 20 \times 3$ subject-background pairs. In Figure 3, we show some examples of backgrounds with bounding boxes and subjects with reference images.

6. Experiments

6.1. Datasets and Implementation Details

We conduct experiments on DreamEditBench dataset and our MureCom dataset. On both datasets, we finetune the pretrained diffusion model for each subject by using its reference images, and then apply the finetuned model to the background images associated with the category of this subject.

We use pretrained diffusion model Stable-Diffusion-Inpainting provided by RunwayML. Its U-Net has 5 additional input channels, whose weights are zero-initialized after restoring the non-inpainting checkpoint. We imple-

Method	Foreground		Overall FID↓
	CLIP _{fg} ↑	DINO _{fg} ↑	
ObjectStitch [43]	0.801	0.599	35.507
PbE [48]	0.768	0.514	34.312
DreamEdit [28]	0.733	0.490	35.654
Ours	0.796	0.648	37.891

Table 1. Quantitative comparison on DreamEditBench dataset.

Method	Foreground		Overall FID↓
	CLIP _{fg} ↑	DINO _{fg} ↑	
ObjectStitch [43]	0.762	0.502	11.935
PbE [48]	0.733	0.414	11.975
DreamEdit [28]	0.657	0.301	12.961
Ours	0.761	0.529	12.299

Table 2. Quantitative comparison on our MureCom dataset.

ment our network using PyTorch 1.11.0 and train our model on Ubuntu 20.04 LTS operating system equipped with one GeForce RTX 3090 GPU, Intel Xeon Silver 4116 CPU, and 32GB of memory.

6.2. Evaluation Metrics

Following PbE [48], we use FID score [18] to evaluate the realism of the whole composite image. Specifically, we collect 200 real images for each category from the Open Images dataset [25], leading to the real image set. For each method, we generate 5 composite images for each background-subject pair, leading to the generated image set. Then, we calculate the FID score by comparing the real image set and generated image set.

Following Dreambooth [39] and DreamEdit [28], we use DINO [5] and CLIP-I [36] scores to evaluate the fidelity of foreground. These scores measure the similarity between the generated foreground and the foregrounds in reference images. CLIP-I (*resp.*, DINO) calculates the average cosine similarity between the embeddings of the generated and real images based on CLIP (*resp.*, ViT-S/16 DINO) embedding. Specifically, for each background-subject pair, we have five generated composite images. Firstly, the foreground of each generated image is evaluated against the foregrounds of all reference images to obtain scores. These scores are then averaged. Finally, the results of the five generated images are averaged to determine the outcome for the subject-background pair. Compared with CLIP-I, DINO is designed to distinguish between different subjects with similar textual descriptions, which can better capture the unique features of each subject.

Number	Foreground	
	CLIP _{fg} ↑	DINO _{fg} ↑
1	0.745	0.488
2	0.756	0.519
3	0.758	0.526
4	0.760	0.531
5	0.761	0.529

Table 3. Quantitative evaluation of the impact of number of reference images on our MureCom dataset.

6.3. Comparison with Baselines

We compare our method with PbE [48], ObjectStitch [43], DreamEdit [28]. For DreamEdit, we finetune the pretrained stable diffusion model v1.4 for each subject. For inference, we utilize GLIGEN as an initialization method. Then, the finetuned model is employed to fill in the bounding box of the background. The result is segmented and a new mask is extracted as the input of next round, which is repeated for five times. For PbE, we use the released model pretrained on Open Images dataset for evaluation. For ObjectStitch, we reimplement the model, train it on Open Images dataset, and use the trained model for evaluation.

The results on DreamEditBench dataset are reported in Tab. 1 and the results on MureCom are reported in Tab. 2. We can see that for DINO metrics, our method achieves the highest scores, followed by ObjectStitch, PbE, and Dreamedit, respectively. This suggests that our generated results are more similar to the reference, and better preserve details than the other methods. ObjectStitch and PbE can only ensure the same semantic category instead of similar finer details. Meanwhile, Dreamedit performs poorly and struggles to generate ideal results for many challenging backgrounds. For CLIP metrics, Our method outperforms PbE and Dreamedit but falls behind ObjectStitch. One reason is that CLIP is less capable of distinguishing the differences between different subjects with highly similar text descriptions compared with DINO. Besides, as mentioned in Section 4, the pretrained inpainting diffusion model is trained with global text prompt, while we use the description of inpainted object as text prompt. When the bounding box is very small, the model is prone to generate nothing in the bounding box. Our proposed remedy of image cropping can partially solve this problem, but there still exist failure cases with nothing generated in the bounding box. For FID metrics, DreamEdit and our method perform worse. The poor performance of DreamEdit is attributed to its inability to generate satisfactory results for many challenging backgrounds, leading to breakdowns in the final inference results. While our method’s subpar results are partially caused by the reason mentioned above.

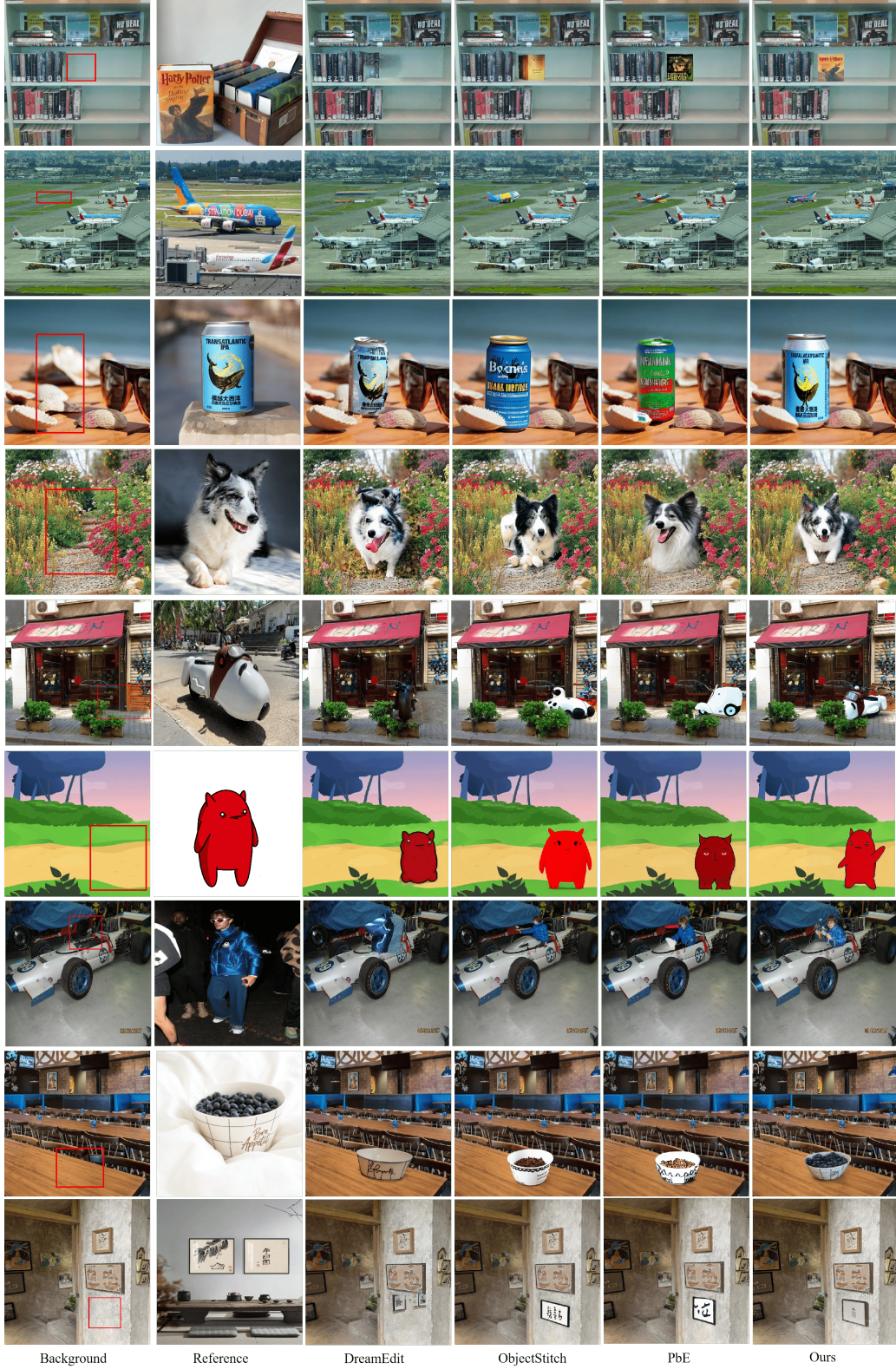


Figure 4. Visualization comparison of different methods. In each row, we show the background image with bounding box, one reference image of subject, and the results of DreamEdit [28], ObjectStitch [43], PbE [48], and our method.

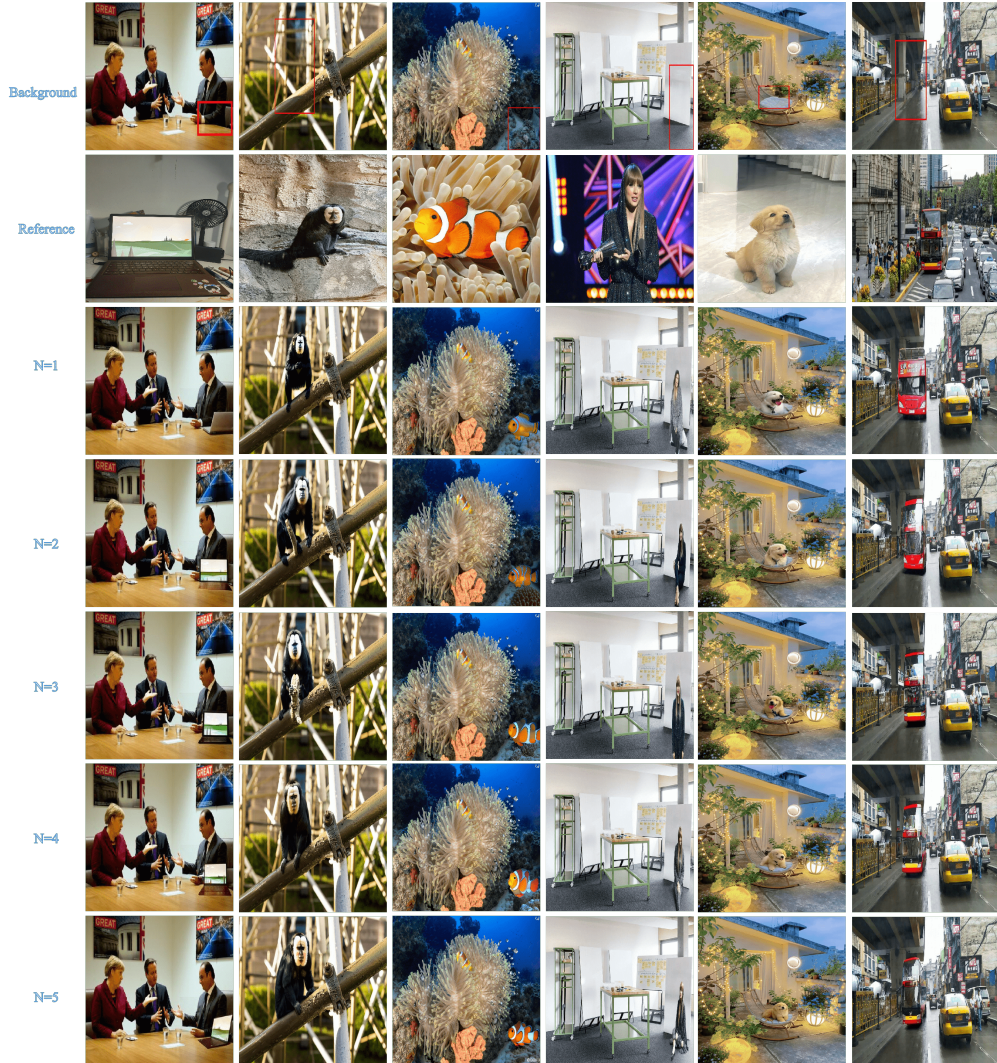


Figure 5. Visualization results using different numbers of reference images per subject. In each column, we show the background image with bounding box, one reference image of subject, and our results.

The visual comparison is shown in Figure 4. We show the background image with bounding box, one reference image of the subject, the generated composite images from DreamEdit, ObjectStitch, PbE, and our method. We observe that the results generated by PbE and ObjectStitch are realistic with the foreground objects belonging to the same semantic category as the subject. However, for the subjects with rich details, the generated foreground objects are very unlike the subject, with many appearance and textual details altered. For DreamEdit, it performs reasonably well in relatively simpler backgrounds (row 3, 4, 6). However, in the case of more challenging backgrounds, Dreamedit exhibits significant limitations and struggles to achieve desired changes (row 1, 2, 5, 7, 9). Our approach can not only achieve results that are more similar to the reference,

preserving more colors, patterns and textures (row 1-3, 8, 9), but also exhibit better adaptability to more challenging backgrounds. The poses of generated foregrounds are more geometrically and semantically compatible with the background, enhancing the overall coherence in complex background settings (row 5, 6, 7).

6.4. The Number of Reference Images

Recall that we use 5 reference images for each subject by default. In this section, we investigate the impact of the number of reference images. We conduct experiments using various numbers of reference images, ranging from 1 to 5. As indicated by Tab. 3, there is a general upward trend in the scores of Clip and Dino with an increasing number of reference images. However, it is difficult to compare

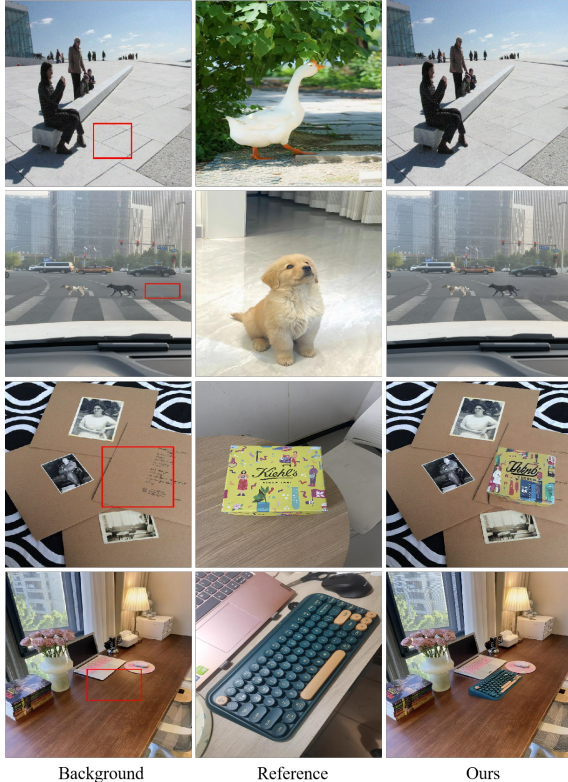


Figure 6. The failure cases of our method.

the numerical performance between using 4 or 5 reference images. This could be attributed to the fact that for some simple backgrounds, the provided 4 reference images are already sufficient to capture the necessary angles and positions. However, for other backgrounds, even with 5 reference images, it may not be enough to learn appropriate poses and angles that adapt well to those backgrounds, indicating a need for additional reference images. As shown in Fig. 5, the results are generally getting better as the number of reference images increases. Firstly, incorporating more references enables the model to learn from a broader range of perspectives, resulting in a more comprehensive understanding of details (column 2, 3, 6). Secondly, by leveraging an increased number of references, the model gains access to additional information on how the subject interacts with and adapts to the background. Consequently, during the generation process, it exhibits improved performance even in more challenging locations (column 1, 4, 5).

6.5. Limitation

We provide some failure cases of our method in Figure 6. As mentioned in Section 4, when the bounding box is very small, our method may fail to generate the object in the bounding box (row 1, 2). Additionally, for the subjects with delicate details (e.g., texts and patterns on the box and

keyboard), our model cannot exactly maintain these delicate details. In these cases, the baseline methods also fail to produce the composite images with all details perfectly preserved. This is still a very critical issue for generative image composition methods.

7. Conclusion

In this paper, we have proposed an embarrassingly simple baseline for image composition, that is, finetuning the pretrained text-guided inpainting model on a few reference images of one subject. We have also contributed a new dataset named MureCom, which could facilitate the research on multi-reference image composition.

References

- [1] Foreground object search by distilling composite image feature. In *ICCV*, 2023. 4
- [2] Smartbrush: Text and shape guided object inpainting with diffusion model. In *CVPR*, 2023. 3
- [3] Yuval Alaluf, Omer Tov, Ron Mokady, Rinon Gal, and Amit H. Bermano. HyperStyle: Stylegan inversion with hypernetworks for real image editing. *CVPR*, 2021. 3
- [4] Zhongyun Bao, Chengjiang Long, Gang Fu, Daquan Liu, Yuanzhen Li, Jiaming Wu, and Chunxia Xiao. Deep image-based illumination harmonization. In *CVPR*, 2022. 2
- [5] Mathilde Caron, Hugo Touvron, Ishan Misra, Hervé Jégou, Julien Mairal, Piotr Bojanowski, and Armand Joulin. Emerging properties in self-supervised vision transformers. In *ICCV*, 2021. 5
- [6] Bor-Chun Chen and Andrew Kae. Toward realistic image compositing with adversarial learning. In *CVPR*, 2019. 2
- [7] Jooyoung Choi, Yunjey Choi, Yunji Kim, Junho Kim, and Sung-Hoon Yoon. Custom-edit: Text-guided image editing with customized diffusion models. *ArXiv*, abs/2305.15779, 2023. 3
- [8] Wenyan Cong, Xinhao Tao, Li Niu, Jing Liang, Xuesong Gao, Qihao Sun, and Liqing Zhang. High-resolution image harmonization via collaborative dual transformations. In *CVPR*, 2021. 2
- [9] Wenyan Cong, Jianfu Zhang, Li Niu, Liu Liu, Zhixin Ling, Weiyuan Li, and Liqing Zhang. DoveNet: Deep image harmonization via domain verification. In *CVPR*, 2020. 2
- [10] Xiaodong Cun and Chi-Man Pun. Improving the harmony of the composite image by spatial-separated attention module. *IEEE Transactions on Image Processing*, 29:4759–4771, 2020. 2
- [11] Rinon Gal, Yuval Alaluf, Yuval Atzmon, Or Patashnik, Amit H. Bermano, Gal Chechik, and Daniel Cohen-Or. An image is worth one word: Personalizing text-to-image generation using textual inversion. *ArXiv*, abs/2208.01618, 2022. 3
- [12] Rinon Gal, Moab Arar, Yuval Atzmon, Amit H. Bermano, Gal Chechik, and Daniel Cohen-Or. Encoder-based domain tuning for fast personalization of text-to-image models. *ArXiv*, abs/2302.12228, 2023. 3

- [13] Jing Gu, Yilin Wang, Nanxuan Zhao, Tsu-Jui Fu, Wei Xiong, Qing Liu, Zhifei Zhang, He Zhang, Jianming Zhang, Hyun-Sun Jung, and Xin Wang. Photoswap: Personalized subject swapping in images. *ArXiv*, abs/2305.18286, 2023. 3
- [14] Julian Jorge Andrade Guerreiro, Mitsuru Nakazawa, and Björn Stenger. Pct-net: Full resolution image harmonization using pixel-wise color transformations. In *CVPR*, 2023. 2
- [15] Zonghui Guo, Dongsheng Guo, Haiyong Zheng, Zhaorui Gu, Bing Zheng, and Junyu Dong. Image harmonization with transformer. In *ICCV*, 2021. 2
- [16] Zonghui Guo, Haiyong Zheng, Yufeng Jiang, Zhaorui Gu, and Bing Zheng. Intrinsic image harmonization. In *CVPR*, 2021. 2
- [17] Yucheng Hang, Bin Xia, Wenming Yang, and Qingmin Liao. SCS-Co: Self-consistent style contrastive learning for image harmonization. In *CVPR*, 2022. 2
- [18] Martin Heusel, Hubert Ramsauer, Thomas Unterthiner, Bernhard Nessler, and Sepp Hochreiter. Gans trained by a two time-scale update rule converge to a local nash equilibrium. In *NIPS*, 2017. 5
- [19] Jonathan Ho, Ajay Jain, and Pieter Abbeel. Denoising diffusion probabilistic models. In *NIPS*, 2020. 3
- [20] Yan Hong, Li Niu, and Jianfu Zhang. Shadow generation for composite image in real-world scenes. In *AAAI*, 2022. 1, 2
- [21] Yifan Jiang, He Zhang, Jianming Zhang, Yilin Wang, Zhe Lin, Kalyan Sunkavalli, Simon Chen, Sohrab Amirghodsi, Sarah Kong, and Zhangyang Wang. Ssh: A self-supervised framework for image harmonization. In *ICCV*, 2021. 2
- [22] Zhanhan Ke, Chunyi Sun, Lei Zhu, Ke Xu, and Rynson W.H. Lau. Harmonizer: Learning to perform white-box image and video harmonization. In *ECCV*, 2022. 2
- [23] Sumith Kulal, Tim Brooks, Alex Aiken, Jiajun Wu, Jimei Yang, Jingwan Lu, Alexei A. Efros, and Krishna Kumar Singh. Putting people in their place: Affordance-aware human insertion into scenes. In *CVPR*, 2023. 2, 3
- [24] Nupur Kumari, Bin Zhang, Richard Zhang, Eli Shechtman, and Jun-Yan Zhu. Multi-concept customization of text-to-image diffusion. In *CVPR*, 2023. 3
- [25] Alina Kuznetsova, Hassan Rom, Neil Alldrin, Jasper Uijlings, Ivan Krasin, Jordi Pont-Tuset, Shahab Kamali, Stefan Popov, Matteo Mallocci, Alexander Kolesnikov, et al. The open images dataset v4: Unified image classification, object detection, and visual relationship detection at scale. *IJCV*, 2020. 5
- [26] Donghoon Lee, Sifei Liu, Jinwei Gu, Ming-Yu Liu, Ming-Hsuan Yang, and Jan Kautz. Context-aware synthesis and placement of object instances. In *NIPS*, 2018. 2
- [27] Dongxu Li, Junnan Li, and Steven Hoi. Blip-diffusion: Pre-trained subject representation for controllable text-to-image generation and editing. *ArXiv*, abs/2305.14720, 2023. 3
- [28] Tianle Li, Max Ku, Cong Wei, and Wenhui Chen. Dreamedit: Subject-driven image editing. *arXiv preprint arXiv:2306.12624*, 2023. 1, 2, 3, 4, 5, 6
- [29] Jingtang Liang, Xiaodong Cun, and Chi-Man Pun. Spatial-separated curve rendering network for efficient and high-resolution image harmonization. *ECCV*, 2022. 2
- [30] Chen-Hsuan Lin, Ersin Yumer, Oliver Wang, Eli Shechtman, and Simon Lucey. ST-GAN: spatial transformer generative adversarial networks for image compositing. In *CVPR*, 2018. 2
- [31] Jun Ling, Han Xue, Li Song, Rong Xie, and Xiao Gu. Region-aware adaptive instance normalization for image harmonization. In *CVPR*, 2021. 2
- [32] Daquan Liu, Chengjiang Long, Hongpan Zhang, Hanning Yu, Xinzhi Dong, and Chunxia Xiao. ARShadowGAN: Shadow generative adversarial network for augmented reality in single light scenes. In *CVPR*, 2020. 2
- [33] Sheng Liu, Cong Phuoc Huynh, Cong Chen, Maxim Arap, and Raffay Hamid. Lemart: Label-efficient masked region transform for image harmonization. In *CVPR*, 2023. 2
- [34] Li Niu, Wenyan Cong, Liu Liu, Yan Hong, Bo Zhang, Jing Liang, and Liqing Zhang. Making images real again: A comprehensive survey on deep image composition. *ArXiv*, abs/2106.14490, 2021. 1, 2
- [35] Patrick Pérez, Michel Gangnet, and Andrew Blake. Poisson image editing. *SIGGRAPH*, 2003. 2
- [36] Alec Radford, Jong Wook Kim, Chris Hallacy, Aditya Ramesh, Gabriel Goh, Sandhini Agarwal, Girish Sastry, Amanda Askell, Pamela Mishkin, Jack Clark, et al. Learning transferable visual models from natural language supervision. In *ICML*, 2021. 5
- [37] Xuqian Ren and Yifan Liu. Semantic-guided multi-mask image harmonization. In *ECCV*, 2022. 2
- [38] Robin Rombach, A. Blattmann, Dominik Lorenz, Patrick Esser, and Björn Ommer. High-resolution image synthesis with latent diffusion models. In *CVPR*, 2022. 3
- [39] Nataniel Ruiz, Yuanzhen Li, Varun Jampani, Yael Pritch, Michael Rubinstein, and Kfir Aberman. Dreambooth: Fine tuning text-to-image diffusion models for subject-driven generation. In *CVPR*, 2023. 1, 3, 4, 5
- [40] Yujun Shen, Jinjin Gu, Xiaoou Tang, and Bolei Zhou. Interpreting the latent space of gans for semantic face editing. *CVPR*, 2019. 3
- [41] Yichen Sheng, Jianming Zhang, and Bedrich Benes. SSN: Soft shadow network for image compositing. *CVPR*, 2021. 2
- [42] Konstantin Sofiiuk, Polina Popenova, and Anton Konushin. Foreground-aware semantic representations for image harmonization. In *WACV*, 2021. 2
- [43] Yi-Zhe Song, Zhifei Zhang, Zhe L. Lin, Scott D. Cohen, Brian L. Price, Jianming Zhang, Soo Ye Kim, and Daniel G. Aliaga. Objectstitch: Generative object compositing. In *CVPR*, 2023. 1, 2, 3, 5, 6
- [44] Yi-Hsuan Tsai, Xiaohui Shen, Zhe Lin, Kalyan Sunkavalli, Xin Lu, and Ming-Hsuan Yang. Deep image harmonization. In *CVPR*, 2017. 1, 2
- [45] Ke Wang, Michaël Gharbi, He Zhang, Zhihao Xia, and Eli Shechtman. Semi-supervised parametric real-world image harmonization. In *CVPR*, 2023. 2
- [46] Yuxiang Wei, Yabo Zhang, Zhilong Ji, Jinfeng Bai, Lei Zhang, and Wangmeng Zuo. ELITE: Encoding visual concepts into textual embeddings for customized text-to-image generation. *ArXiv*, abs/2302.13848, 2023. 3

- [47] Ben Xue, Shenghui Ran, Quan Chen, Rongfei Jia, Binqiang Zhao, and Binqiang Zhao. Dccf: Deep comprehensible color filter learning framework for high-resolution image harmonization. In *ECCV*, 2022. [2](#)
- [48] Binxin Yang, Shuyang Gu, Bo Zhang, Ting Zhang, Xuejin Chen, Xiaoyan Sun, Dong Chen, and Fang Wen. Paint by example: Exemplar-based image editing with diffusion models. In *CVPR*, 2023. [1](#), [2](#), [3](#), [5](#), [6](#)
- [49] Fangneng Zhan, Hongyuan Zhu, and Shijian Lu. Spatial fusion GAN for image synthesis. In *CVPR*, 2019. [2](#)
- [50] Bo Zhang, Yuxuan Duan, Jun Lan, Yan Hong, Huijia Zhu, Weiqiang Wang, and Li Niu. Controlcom: Controllable image composition using diffusion model. *arXiv:2308.10040*, 2023. [1](#)
- [51] He Zhang, Jianming Zhang, Federico Perazzi, Zhe Lin, and Vishal M Patel. Deep image compositing. In *WACV*, 2021. [2](#)
- [52] Lingzhi Zhang, Tarmily Wen, and Jianbo Shi. Deep image blending. In *WACV*, 2019. [1](#), [2](#), [3](#)
- [53] Siyuan Zhou, Liu Liu, Li Niu, and Liqing Zhang. Learning object placement via dual-path graph completion. In *ECCV*, 2022. [2](#)